

## DIFFERENT CONCENTRATIONS OF SODIUM HYDROXIDE CAUSTIC LEACHING OF Cr<sup>6+</sup> FOR REFINEMENT OF CALCIUM SOURCE FROM DENTAL MOULD WASTE

Nur Liyana Mohd Rosli<sup>1,2</sup> and Yanny Marliana Baba Ismail<sup>1\*</sup>

<sup>1</sup> Biomaterials Niche Group, School of Materials and Mineral Resources Engineering, Engineering Campus, Universiti Sains Malaysia, 14300 Nibong Tebal, Penang, Malaysia.

<sup>2</sup> Advance Material Processing & Design, Faculty of Mechanical Engineering Technology, Universiti Malaysia Perlis, Kampus Pauh Putra, 02600 Arau, Perlis, Malaysia.

\* [yannymarliana@usm.my](mailto:yannymarliana@usm.my)

---

**Abstract.** Dental mould is a component used in making the model structures of patient-specific dentures in treating tooth defects. It will be disposed of once the patient obtains their dentures. Dumping these non-biodegradable wastes into the landfills, particularly the green dental mould waste (DMW-type 3) which is characterized as calcium sulphate dihydrate (CaSO<sub>4</sub>.2H<sub>2</sub>O) containing chromium. CaSO<sub>4</sub>.2H<sub>2</sub>O can produce odorous hydrogen sulfide gas as well as introduce toxic chromium into the soil. The current study aimed to process DMW via alkaline roasting followed by caustic leaching to remove chromium and subsequently convert it into high purity calcium hydroxide (Ca(OH)<sub>2</sub>). The ground DMW powder was mixed with sodium carbonate (Na<sub>2</sub>CO<sub>3</sub>) and roasted at 1000°C for an hour. The roasted samples were then proceeded with caustic leaching using 5, 7 and 10M of sodium hydroxide (NaOH). The effect of different concentrations of NaOH on chromium removal was investigated. Our finding showed that chromium could be efficiently leached out up to 94% using 7M NaOH. The white residue powder indicated the efficiency of chromium removal, which was then confirmed by X-ray Fluorescence (XRF) analysis. This is supported by X-ray Diffraction (XRD) analysis, demonstrating the formation of the portlandite (Ca(OH)<sub>2</sub>) phase. The synthesized Ca(OH)<sub>2</sub> powder observed under Field Emission Scanning Electron Microscopy (FESEM) showed highly agglomerated with the presence of needle-shape or fibrous-like particles. Transforming this calcium-rich DMW into Ca(OH)<sub>2</sub>, which then can be used as a source of raw material in making bone substitute material is thought to be one of the sustainable approaches in preserving our environment.

**Keywords:** dental mould waste (DMW), calcium sulphate dihydrate, chromium removal, alkaline roasting, caustic leaching

---

### Article Info

Received 3<sup>rd</sup> November 2021

Accepted 26<sup>th</sup> March 2022

Published 20<sup>th</sup> April 2022

Copyright Malaysian Journal of Microscopy (2022). All rights reserved.

ISSN: 1823-7010, eISSN: 2600-7444

## Introduction

Dental mould is a model or working cast (gypsum cast) that is typically used in making dentures for dental restoration of defect teeth [1]. The dental mould is specifically made for an individual patient and will be discarded after dentures were produced. Generally, dental mould is fabricated using type 3 dental stone which is frequently coloured as green resulting from the presence of chromium in the dental mould composition. The main ingredient of dental stone is calcium sulphate dihydrate ( $\text{CaSO}_4 \cdot 2\text{H}_2\text{O}$ ), commonly known as gypsum. The mixture of dental stone/water ratio is typically prepared according to manufacturer recommendations which would influence the setting time and the presence of pore on the surface. Hand mixing, vibration and vacuum are common methods for mixing the mixture. Utilizing fast-setting gypsum for dental stones improves the setting time which is beneficial for reproducibility in the fabrication of dental gypsum products (dental mould) [2].

Large quantities of  $\text{CaSO}_4 \cdot 2\text{H}_2\text{O}$  are consumed for routine dental work in creating a model of the dental or oral structures, which subsequently contribute to large amount of waste that are disposed into landfills. Chemically the decomposition of gypsum waste in landfills can result in sulfate content in gypsum reacting with other compounds found in landfills [3]. Dental stone is reported as non-degradable gypsum; hence the discarded dental mould wastes would be a significant threat to humans and the surrounding ecosystem if not properly disposed of. In fact, when dumping any gypsum-based product in an anaerobic moist environment, hydrogen sulfide gas would be released an odour similar to that of stinky rotten eggs [4]. This bad smell gas is classified as toxic and inflammable, and thus has been restricted due to environmental health concerns [5]. The situation can be worsened because the released hydrogen sulfide gas may cause long-term effects such as headaches, tiredness, and poor psycho-motor function [6]. Therefore, the crucial issue caused by this type of waste is that the waste materials are typically discharged directly into ecosystems without proper treatment and thus need much more attention. Hence, one option to minimize this issue is to recycle or re-use the dental mould waste (DMW) into functional products, rather than disposing it into landfills. Another challenge in this work would be to eliminate the presence of chromium content in the DMW-type 3 waste prior to the synthesis of calcium source powder. The green-coloured pigment has to be removed in order to be acceptable as bone substitute material.

Previous studies explored several methods for the removal of chromium, among which are calcium roasting [7], alkaline roasting-water leaching [8], alkaline leaching [9] and acidic leaching [10]. However, to the best of our knowledge, limited studies had focused on the issue of non-degradable gypsum based DMW. To date, there is no proposed method for the removal of chromium from DMW being reported. Therefore, alternative processing routes in removing the chromium in  $\text{CaSO}_4 \cdot 2\text{H}_2\text{O}$  while producing a potential calcium source is proposed in this work using a roasting-leaching process. The incorporation of an alkali salt of  $\text{Na}_2\text{CO}_3$  into  $\text{CaSO}_4 \cdot 2\text{H}_2\text{O}$  containing-chromium during roasting, would lead to oxidation. This reaction is postulated to oxidize insoluble trivalent chromium ( $\text{Cr}^{3+}$ ) to hexavalent chromium ( $\text{Cr}^{6+}$ ) while producing water-soluble sodium chromate ( $\text{Na}_2\text{CrO}_4$ ) [11]. Subsequently, to completely remove the chromium substance, caustic soda of  $\text{NaOH}$  can be used to solubilise  $\text{Na}_2\text{CrO}_4$ . Hence, the green filtrate which represents the soluble  $\text{Na}_2\text{CrO}_4$  will be removed during this caustic leaching.

Thus, the present study aims to convert the calcium-rich DMW into a potential  $\text{Ca}(\text{OH})_2$  via alkaline roasting and subsequently caustic leaching. For this purpose, samples were roasted with the presence of  $\text{Na}_2\text{CO}_3$  and subsequently leached with different molar concentrations (5,

7 and 10 M of NaOH). The effect of the molar concentrations of NaOH on chromium removal efficiency, phase composition, crystal structure and lattice parameters, morphology and the elemental composition of the powder particles were investigated.

## Materials and Methods

In the present work, the DMW was collected from Advanced Medical and Dental Institute (AMDI), Universiti Sains Malaysia (USM) in Kepala Batas, Penang. The dental mould collected was a type 3 dental stone.

**Sample preparation.** The green-coloured dental mould wastes were initially cleaned, crushed, and ground into finer powder using a high energy planetary ball mill (PM 100, Retsch) for 1 hour at ambient conditions. The rotational speed was set at 300 rpm with a ball-to-powder ratio of 2:1 and a deionized water-to-powder ratio of 4:1. This milled powder was then mixed with Na<sub>2</sub>CO<sub>3</sub> (Merck, 99.50% pure) with 2:1 ratio of alkali salt-to-Cr<sub>2</sub>O<sub>3</sub>. The content of Cr<sub>2</sub>O<sub>3</sub> was determined by XRF. The prepared powder was placed in an alumina crucible and roasted in a Lenton furnace at 1000 °C for 1 hour with a heating rate of 5 °C/min. Caustic leaching solution was prepared by dissolving a pre-calculated amount of NaOH (Merck, 99.00% pure) for 5, 7 and 10 M NaOH into 1 litre of deionized water. The roasted sample was mixed in 100 mL of prepared NaOH solution and continuously stirred for an hour. The solution was then filtered and washed five times with deionized water. The filtered cake was dried in the oven at 100 °C for 24 hours prior to characterization. The prepared samples are classified according to the processing method as shown in Table 1.

**Table 1. Sample classification and processing parameters.**

Sample classification	Samples Code	Processing Method	Salt
As-milled	CS	High energy wet planetary ball milling	-
Roasted	CSNC	Alkaline roasting	Na <sub>2</sub> CO <sub>3</sub>
Leaching residue	CSNC5	Alkaline roasting- caustic leaching	Na <sub>2</sub> CO <sub>3</sub> - 5M NaOH
	CSNC7	Alkaline roasting- caustic leaching	Na <sub>2</sub> CO <sub>3</sub> - 7M NaOH
	CSNC10	Alkaline roasting- caustic leaching	Na <sub>2</sub> CO <sub>3</sub> - 10M NaOH

**Material characterizations.** The phase composition, crystal structure and lattice parameters of as-milled DMW, roasted samples and leaching residue samples with different molar ratios of NaOH were determined by X-ray diffraction (XRD; Bruker D2 Phaser XRD, Germany). XRD was performed with diffraction angles  $2\theta$  of  $10^\circ \leq 2\theta \leq 80^\circ$  using Cu K $\alpha$  radiation ( $\lambda = 1.5418 \text{ \AA}$ ). The XRD data were analyzed using PANalytical X'pert Highscore software. The XRD patterns were compared to the standard ICSD database patterns. Rietveld refinement was used to analyze the samples quantitatively. Additionally, the chemical composition of all prepared samples was examined using X-ray fluorescence (XRF; MiniPal4 X-ray Fluorescent Spectrometer, PANalytical, United Kingdom). Field emission scanning electron microscope (FESEM; Zeiss Supra™ Gemini 35 VP) equipped with an energy-

dispersive X-ray spectroscope (EDX) was used to examine the morphological features and elemental composition of the samples.

## Results and Discussion

**Physico-chemical analyses.** Figure 1 shows the XRD pattern of as-milled DMW (CS) and roasted samples (CSNC). The XRD pattern of as-milled CS confirmed that the main phase was identified as gypsum, which corresponds to  $\text{CaSO}_4 \cdot 2\text{H}_2\text{O}$  with ICSD: 98-001-1992. The phase formed when plaster powder was merely mixed with water to make the denture mould.

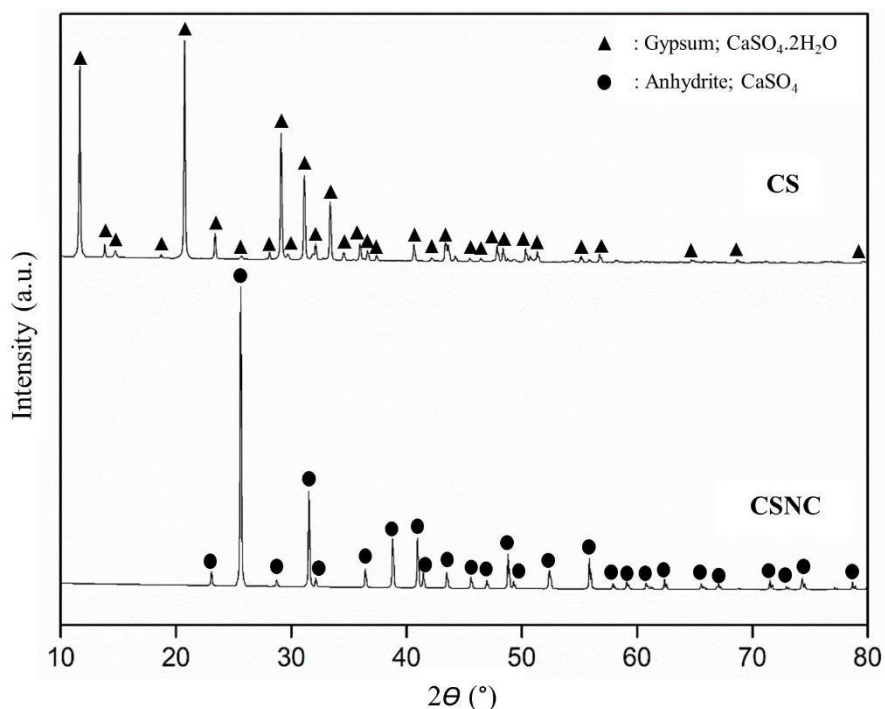
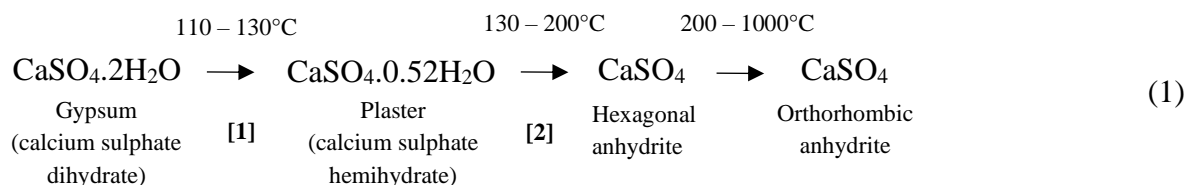


**Figure 1. XRD analysis of as-milled DMW and roasted sample.**

The calcium sulfate (VI) dihydrate phase can be observed by the presence of six major diffraction peaks: (020), (021), (130), (04-1), (22-1) and (220) at positions ( $2\theta$ ) of  $11.63^\circ$ ,  $20.73^\circ$ ,  $23.41^\circ$ ,  $29.11^\circ$ ,  $31.11^\circ$  and  $33.39^\circ$ , respectively. The CS sample was crystallized in a monoclinic structure and belongs to space group  $C 1 2/c 1$ . The lattice parameters resulted as  $a \neq b \neq c$  and  $\alpha \neq \beta = \gamma = 90^\circ$ , where  $a = 6.287 \text{ \AA}$ ,  $b = 15.202 \text{ \AA}$ ,  $c = 5.679 \text{ \AA}$  and  $\beta = 114.170^\circ$ . These values were close to corresponding data of  $\text{CaSO}_4 \cdot 2\text{H}_2\text{O}$  crystal structure reported from the previous study [12].

It was also observed that, after roasting the CS had transformed CSNC into single-phase  $\text{CaSO}_4$ , with major peaks at (200), (021), (220), (221), (023) and (223) and  $2\theta \approx 25.54^\circ$ ,  $31.42^\circ$ ,  $38.74^\circ$ ,  $40.92^\circ$ ,  $49.92^\circ$  and  $55.89^\circ$ . Peak position and lattice parameters of CSNC were indexed corresponding to anhydrite,  $\text{CaSO}_4$  (ICSD: 98-001-0224). The dehydration of  $\text{CaSO}_4 \cdot 2\text{H}_2\text{O}$  produces anhydrous  $\text{CaSO}_4$  by two endothermic decomposition reactions during roasting as described in the following reaction [13]:



The alkaline roasting then changed to orthorhombic structure and coordinates in the space group  $C m c m$ . Refinement of the lattice parameters of the  $\text{CaSO}_4$ , resulted in the values of  $a \neq b \neq c$  and  $\alpha = \beta = \gamma = 90^{\circ}$ , where  $a = 6.970 \text{ \AA}$ ,  $b = 6.230 \text{ \AA}$ ,  $c = 6.980 \text{ \AA}$  and  $\beta = 90.000^{\circ}$ . This transformation caused the monoclinic gypsum crystals to become unstable and consequently undergoes restructuring to an orthorhombic crystal of anhydrite as presented in Table 2 [14]. Thus, the results showed that heating gypsum at higher temperatures resulted in complete dehydration, which was influenced by the loss of water crystallization during roasting [15]. Additionally, the  $\text{CaSO}_4 \cdot 2\text{H}_2\text{O}$  containing-chromium was also simultaneously reacting with  $\text{Na}_2\text{CO}_3$  throughout roasting at  $1000^{\circ}\text{C}$ , resulting in the formation of the  $\text{Na}_2\text{CrO}_4$  phase which is a soluble compound. At temperatures above  $900^{\circ}\text{C}$ ,  $\text{Cr}^{3+}$  diffused outward of the spinel lattice and reacted with  $\text{Na}^+$  from the alkali salt [16-17]. The formation of  $\text{Na}_2\text{CrO}_4$  under this oxidative condition is given by the following reactions [18]:

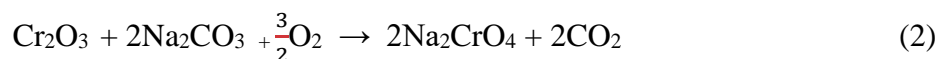


Figure 2 shows the XRD patterns of the leached residue samples of 5, 7 and 10 M NaOH concentrations. The XRD analysis revealed similar peak profiles to portlandite ( $\text{Ca}(\text{OH})_2$ ) corresponding to ICSD: 98-005-8841. The  $2\theta$  of the main peaks were detected at  $18.23^{\circ}$ ,  $28.87^{\circ}$ ,  $34.36^{\circ}$ ,  $47.55^{\circ}$ ,  $51.16^{\circ}$  and  $54.76^{\circ}$  corresponding to lattice plane of (001), (010), (012), (110) and (111), indicating the main phase of  $\text{Ca}(\text{OH})_2$ .

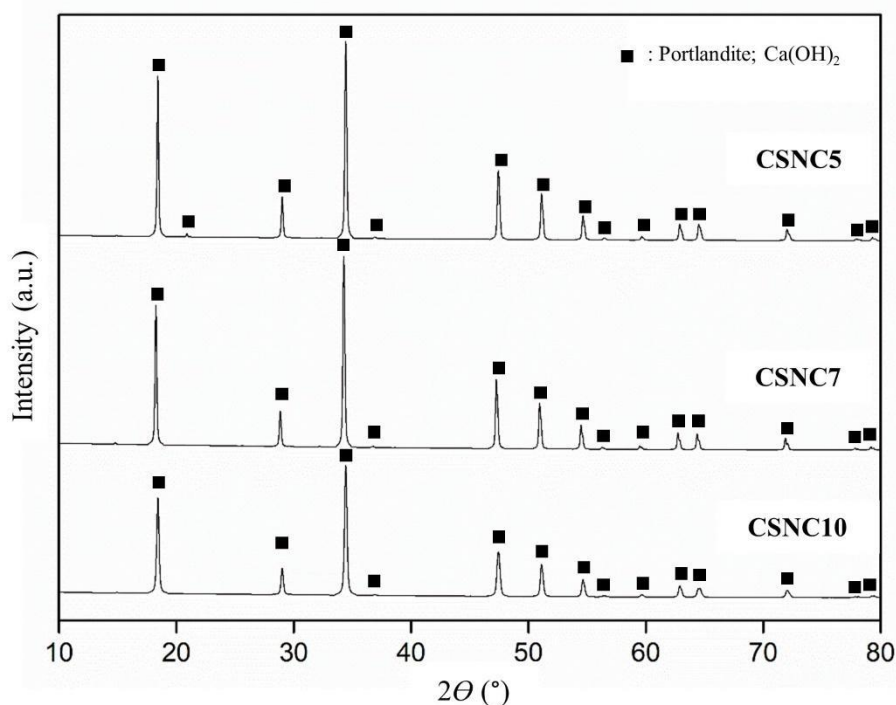
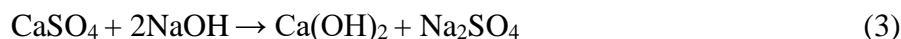


Figure 2. XRD analysis of roasted and leaching residue samples.

The resultant  $\text{Ca(OH)}_2$  after leaching is well crystallized in a hexagonal system with space group P-3 m 1 (Table 2). The lattice parameters are identified as  $a = b \neq c$  and  $\alpha = \beta = 90^\circ$ ;  $\gamma = 120^\circ$ , where  $a = 3.568 \text{ \AA}$ ,  $b = 3.568 \text{ \AA}$ ,  $c = 4.863 \text{ \AA}$  and  $\beta = 90.000^\circ$ . The  $\text{Ca(OH)}_2$  was formed through the reaction of a caustic solution of NaOH with roasted  $\text{CaSO}_4$ . The calcium ion ( $\text{Ca}^{2+}$ ) that dissociated from  $\text{CaSO}_4$  (from reaction Equation 1) then would react with hydroxide ( $\text{OH}^-$ ), forming  $\text{Ca(OH)}_2$  [19]. This reaction results in a white precipitate  $\text{Ca(OH)}_2$  obtained after the filtration process. Along with this reaction, the leaching process also enabled the separation of chromium by removing the soluble  $\text{Na}_2\text{CrO}_4$  through the filtrate [20]. The following equation can be used to describe the caustic leaching:



**Table 2. Lattice parameters and crystallite size of as-milled DMW, roasted and leaching residue samples.**

Samples	Crystal system	<i>a</i> -axis (Å)	<i>b</i> -axis (Å)	<i>c</i> -axis (Å)	<i>c/a</i> ratio	FWHM (°)	Crystallite size (nm)
CS	Monoclinic	6.287	15.2020	5.679	0.903	0.175	51.9
CSNC	Orthorhombic	6.970	6.2300	6.980	1.001	0.092	88.6
CSNC5	Hexagonal	3.568	3.5680	4.895	1.372	0.120	69.8
CSNC7	Hexagonal	3.568	3.5680	4.895	1.372	0.152	54.0
CSNC10	Hexagonal	3.568	3.5680	4.895	1.372	0.203	41.3

The effect of different molar concentrations of NaOH on chromium removal is represented in Figure 3. It is observed that the maximum chromium removal efficiency is obtained by leaching with 7 M NaOH that resulted in 94% removal. On the other hand, only 90% and 92% removal chromium for 5 M and 10 M NaOH concentrations, respectively. The reduction of chromium removal efficiency from 94% to 92% is due to the increase of viscosity in NaOH solution and thus ineffective reaction had occurred. As has been reported in the literature, increasing the viscosity of the NaOH solution through the addition of excess molar concentration of NaOH hindered the oxygen diffusion to the reaction interface [21]. This can be explained due to the decreasing of  $\text{O}_2$  solubility in NaOH solution with the increasing NaOH concentration, similarly, reported by Zhang et al. [9]. In other words,  $\text{Ca(OH)}_2$  solubility might be reduced by the effect of  $\text{OH}^-$  ion action [22]. It is noteworthy to realize that the concentration of NaOH (in molar) had a significant impact on the efficiency of chromium removal.

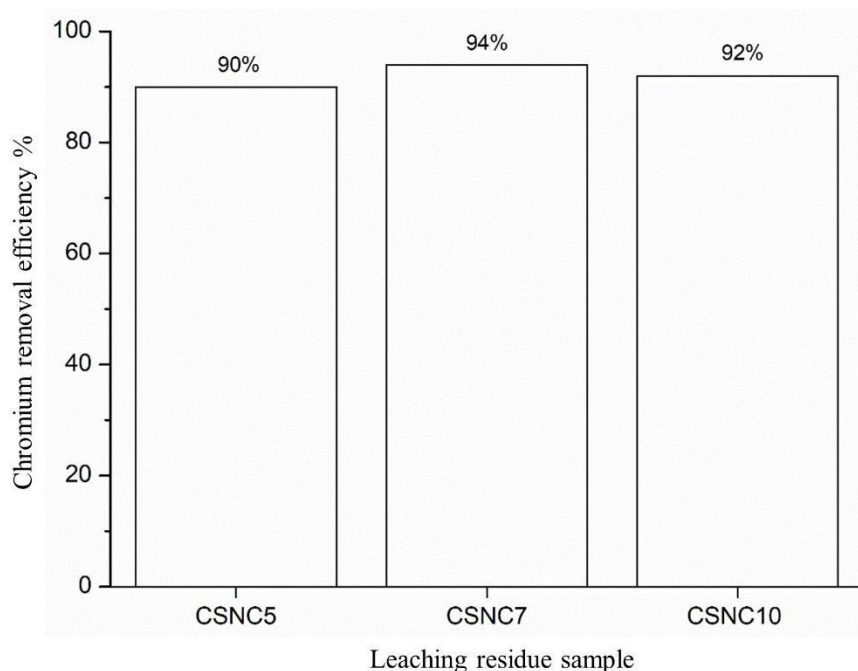


**Figure 3. Effect of different molar concentrations of sodium hydroxide on chromium removal.**

These findings are further supported by XRF analysis. Table 3 shows the major elements of the as-milled DMW, roasted and leaching residue samples detected by XRF. Chemical compositions of samples are mainly composed of sulfur trioxide ( $\text{SO}_3$ ) and calcium oxide (CaO) which makes up the  $\text{CaSO}_4$  as well as alumina ( $\text{Al}_2\text{O}_3$ ), for CS and CSNC samples. It is clear that the  $\text{Cr}_2\text{O}_3$  content decreased consistently, particularly after roasting and leaching. As expected, increment of CaO weight percent would indicate the formation of  $\text{Ca}(\text{OH})_2$  throughout the caustic leaching and stabilizes at a higher molar concentration of NaOH used.

**Table 3. Major elemental composition of as-milled DMW, roasted and leaching residue samples.**

Compound (wt.%)	Sample				
	CS	CSNC	CSNC5	CSNC7	CSNC10
CaO	46.54	38.72	93.07	92.80	92.78
$\text{SO}_3$	50.25	56.03	0.39	0.57	0.75
$\text{Al}_2\text{O}_3$	2.00	3.80	5.50	5.40	5.40
$\text{Fe}_2\text{O}_3$	0.12	0.05	0.22	0.11	0.13
$\text{Cr}_2\text{O}_3$	1.09	0.83	0.11	0.07	0.09

**Morphological and elemental analyses.** FESEM was carried out to examine the morphological changes of DMW or  $\text{CaSO}_4 \cdot 2\text{H}_2\text{O}$  after alkaline roasting and subsequent caustic leaching. The microstructure of the roasted sample shows aggregated grains of randomly

orientated plate-like particles as shown in Figure 4(a). After caustic leaching, the platy particles had transformed to a new form of agglomerate structures as shown in Figure 4(b), (c) and (d). The leaching residue samples appeared as intersecting plate-like structures and it is stacked up more closely as can be seen particularly in Figures 4 (b) and (c). Particle morphology has evolved to an irregular crystal structure without a complete shape. It can be understood that was related to the dissolution-crystallization principle [14].

Additionally, it can be observed that the morphology of leached residue samples had disintegrated to much smaller size of needle-shape or fibrous-like particles with further increased of molar concentration up to 10 M NaOH (Figure 4 (d)). The reduction of size than the microstructure observed in CSNC5 and CSNC7, was attributed to a decrease in solubility caused by higher molarity of NaOH [23]. This clearly indicates that the complete dehydration of  $\text{CaSO}_4 \cdot 2\text{H}_2\text{O}$  and the subsequent dissolution from the reacting ion of NaOH significantly affects the morphology of the powders.

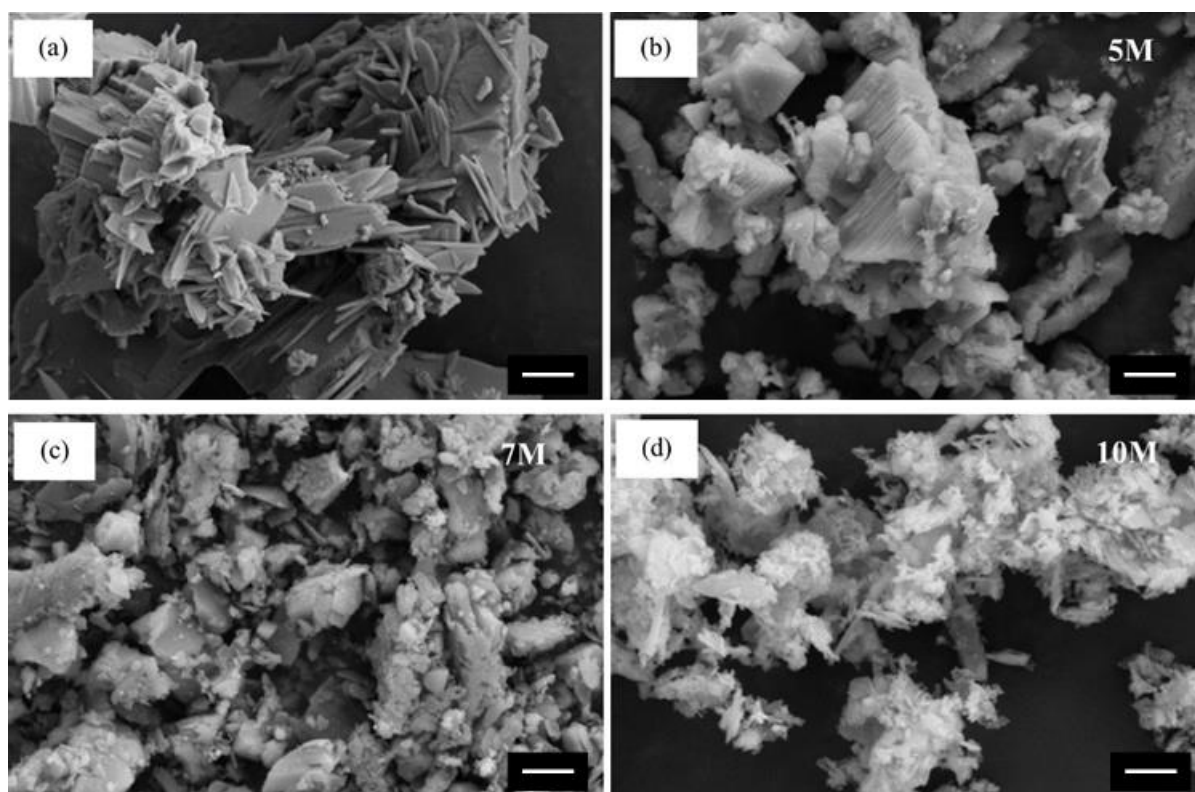


**Figure 4. SEM micrographs of (a) roasted and (b), (c) and (d) leaching residue samples (Magnification = 5000X and scale bar = 2  $\mu\text{m}$ )**

The presence of calcium (Ca), sulfur (S) and chromium (Cr) at the selected area of samples could be differentiated in the form of weight percent by FESEM-EDX (Table 4). The result shows a reduction of chromium weight percent after roasting followed by leaching. This matches with the XRF results with regard to the decreasing weight percent of  $\text{Cr}_2\text{O}_3$ , and for the  $\text{SO}_3$  resulting from the transformation of  $\text{CaSO}_4$  to form  $\text{Ca}(\text{OH})_2$  (Table 3).

**Table 4. EDX analysis of as-milled DMW, roasted, and leaching residue samples.**

Compound (wt.%)	Sample				
	CS	CSNC	CSNC5	CSNC7	CSNC10
Ca	44.41	45.14	52.37	45.82	44.3
S	16.23	16.37	2.86	3.18	2.45
Cr	16.17	15.4	7.01	4.83	5.79
O	21.39	17.41	31.02	35.92	34.31
Na	-	2.65	1.79	1.40	1.71
C	-	1.56	2.62	7.11	9.45
Fe	1.03	0.78	1.13	0.91	1.08
Al	0.77	0.69	1.20	0.82	0.91

## Conclusion

The feasibility of producing  $\text{Ca(OH)}_2$  from discarded DMW was accomplished by alkaline roasting with subsequent NaOH caustic leaching. Chromium removal from the DMW was achieved with optimum efficiency at 94% utilizing 7 M NaOH. Converting DMW into a calcium source via alkaline roasting with subsequent caustic leaching could replace the approach of dumping into landfills. This sustainable approach in minimizing its implications to human health and environmental aspects and providing a new source of  $\text{Ca(OH)}_2$  for various applications, particularly for biomedical applications such as bone and dental substitute materials, would be a potential interest from waste to wealth.

## Acknowledgements

The financial support for this research was provided by Universiti Sains Malaysia Research University Grant (RUI): 1001/PBAHAN/8014143 and the Ministry of Higher Education Malaysia (MOHE).

## Author Contributions

All authors contributed toward data analysis, drafting and critically revising the paper and agree to be accountable for all aspects of the work.

## Disclosure of Conflict of Interest

The authors have no disclosures to declare.

## Compliance with Ethical Standards

The work is compliant with ethical standards.

## References

- [1] Saeed, F., Muhammad, N., Khan, A. S., Sharif, F., Rahim, A., Ahmad, P. & Irfan, M. (2020). Prosthodontics dental materials: From conventional to unconventional. *Mater. Sci. Eng. C.*, 106 110167.
- [2] Kim, J. H., Im, Y. W., Oh, S., Kim, H. W., Lee, J. H. & Lee, H. H. (2019). Characterization of an anti-foaming and fast-setting gypsum for dental stone. *Dent Mater.*, 35 1728–1739.
- [3] Hansen, S. & Sadeghian, P. (2020). Recycled gypsum powder from waste drywalls combined with fly ash for partial cement replacement in concrete. *J. Clean. Prod.*, 274 12278.
- [4] Asabe, R. & Bhansali, M. (2020). Recycling and Reuse of Dental Materials: An Overview. *J. emerg. Technol. Innov.res.*, 7(8) 186–190.
- [5] Amine Laadila, M., LeBihan, Y., Caron, R. F. & Vaneckhaute, C. (2021). Construction, renovation and demolition (CRD) wastes contaminated by gypsum residues: Characterization, treatment and valorization. *Waste Manage.*, 120 125–135.
- [6] Arora, S., Mittal, S. & Dogra, V. (2017). Eco-friendly dentistry: Need of future. An overview. *Journal of Dental and Allied Sciences*, 6(1) 205446.
- [7] Peng, H., Guo, J., Lv, L., Huang, H. & Li, B. (2020). Recovery of chromium by calcium-roasting, sodium-roasting, acidic leaching, alkaline leaching and sub-molten technology: a review. *Environ. Chem. Lett.*, 19(2) 1383-1393.
- [8] Gu, F., Zhang, Y., Peng, Z., Su, Z., Tang, H., Tian, W., Liang, G., Lee, J., Rao, M., Li, G. & Jiang, T. (2019). Selective recovery of chromium from ferronickel slag via alkaline roasting followed by water leaching. *J. Hazard. Mater.*, 374 83–91.
- [9] Zhang, H., Xu, H. Bin, Zhang, X., Zhang, Y. & Zhang, Y. (2014). Pressure oxidative leaching of Indian chromite ore in concentrated NaOH solution. *Hydrometallurgy*, 142 47–55.
- [10] Escudero-Castejón, L., Taylor, J., Sánchez-Segado, S. & Jha, A. (2021). A novel reductive alkali roasting of chromite ores for carcinogen-free Cr<sup>6+</sup>-ion extraction of chromium oxide (Cr<sub>2</sub>O<sub>3</sub>) – A clean route to chromium product manufacturing. *J. Hazard. Mater.*, 403 123589.
- [11] Escudero-Castejon, Lidia, Sanchez-Segado, S., Parirenyatwa, S. & Jha, A. (2016). Formation of Chromium-Containing Molten Salt Phase during Roasting of Chromite Ore with Sodium and Potassium Hydroxides. *J. Manuf. Sci. Eng. Trans.*, 16(4) 215–225.
- [12] Fukami, T., Tahara, S., Nakasone, K. & Yasuda, C. (2015). Synthesis, Crystal Structure, and Thermal Properties of CaSO<sub>4</sub>·2H<sub>2</sub>O Single Crystals. *Int. J. Chem.*, 7(2) 12.
- [13] Engbrecht, D. C. & Hirschfeld, D. A. (2016). Thermal analysis of calcium sulfate

dihydrate sources used to manufacture gypsum wallboard. *Thermochim. Acta.*, 639 173–185.

[14] Huang, W., Ertekin, E., Wang, T., Cruz, L., Dailey, M., DiRuggiero, J. & Kisailus, D. (2020). Mechanism of water extraction from gypsum rock by desert colonizing microorganisms. *Proc. Natl. Acad. Sci.*, 117(20) 10681–10687.

[15] Chen, X., Wu, Q., Gao, J. & Tang, Y. (2021). Hydration characteristics and mechanism analysis of b-calcium sulfate hemihydrate. *Constr Build Mater.*, 296.

[16] Parirenyatwa, S., Escudero-Castejon, L., Sanchez-Segado, S., Hara, Y. & Jha, A. (2016). Comparative study of alkali roasting and leaching of chromite ores and titaniferous minerals. *Hydrometallurgy*, 165 213–226.

[17] Sanchez-Segado, S. & Jha, A. (2013). Physical chemistry of roasting and leaching reactions for chromium chemical manufacturing and its impact on the environment - A review. *Mater. Process Fund.*, 225-236.

[18] Qi, T., Li, X., Liu, G. & Zhou, Q. (2011). Thermodynamics of chromite ore oxidative roasting process Thermodynamics of chromite ore oxidative roasting process. *J. Cent. South Univ.*, 18(1) 83-88

[19] Wang, D., Wang, Q. & Huang, Z. (2020). New insights into the early reaction of NaOH-activated slag in the presence of CaSO<sub>4</sub>. *Compos. B. Eng.*, 198. 108207.

[20] EldougDoug, A. A., Harbi, H. M., Alwael, H. & El-Shahawi, M. S. (2019). Mineral processing: leaching process of chromium and recovery of platinum group elements from Northwestern Saudi Arabian Ophiolitic chromite. *SN Appl. Sci.*, 1 527.

[21] Escudero-Castejon, L., Sanchez-Segado, S., Parirenyatwa, S., Jha, A., L. Escudero-Castejon, S. Sanchez-Segado, S. Parirenyatwa & A. J. (2016). An investigation on the formation of molten salt containing chromium oxide during roasting of chromite ore with sodium and potassium hydroxides. *Advances in Molten Slags, Fluxes, and Salts: Proceedings of the 10th International Conference on Molten Slags, Fluxes and Salts*, 71–78.

[22] Yuan, T., Wang, J. & Li, Z. (2010). Fluid Phase Equilibria Measurement and modelling of solubility for calcium sulfate dihydrate and calcium hydroxide in NaOH / KOH solutions. *Fluid Phase Equilib.*, 297. 129–137.

[23] Inoue, M. & Hirasawa, I. (2013). The relationship between crystal morphology and XRD peak intensity on CaSO<sub>4</sub>·2H<sub>2</sub>O. *J. Cryst. Growth.*, 380. 169–175.